International Journal of Research in Engineering and Science (IJRES)
ISSN (Online): 2320-9364, ISSN (Print): 2320-9356
www.ijres.org Volume 2 Issue 1 ǁ Jan 2014 ǁ PP.01-10

Design and performance of Four-Stage Adsorption System

A.F.M. Mizanur Rahman[1],*, Y. Ueda[1], A. Akisawa[1], T. Miyazaki[2] and B.B. Saha[3,4]

[1]*Nuclear Power and Energy Division, Bangladesh Atomic Energy Commission, Pormanu Bhaban, E-12/A, Sher-e-Bangla Nagar, Agargaon, Dhaka-1207, Bangladesh*
[2]*Faculty of Engineering Sciences, Kyushu University, 6-1 Kasuga-koen, Kasuga-shi, Fukuoka, 816-8580, Japan*
[3]*Mechanical Engineering Departments, Faculty of Engineering, Kyushu University, 744 Motooka, Nishi-ku Fukuoka, 819-0395, Japan*
[4]*International Institute for Carbon-Neutral Energy Research (WPI-I2CNER), Kyushu University, 744 Motooka, Nishi-ku, Fukuoka 819-0395, Japan.*

ABSTRACT : *A design of four-stage adsorption system was proposed to utilize very low temperature waste heat or solar heat. A simulation model for the proposed cycle was developed to analyse the influence of cycle time and driving heat source temperature on the performance of system identifying the specific cooling power (SCP) and coefficient of performance (COP). It was found that the proposed cycle could be driven by waste heat temperature as low as 35°C with the coolant at 30°C. Both SCP and COP of the proposed system is very low at lower heat source temperature, which can be improved through optimization of cycle time with other design parameters.*

Keyword: *Adsorption Cycle, Four-stage, Cycle Time, Simulation, Optimization, Utilization of Waste Heat.*

I. Introduction

Adsorption heat pump is one of the key technology to utilize waste heat or solar heat. It ~~is~~ uses neither ozone layer depleting gases such as CFCs/HCFCs, nor fossil fuel or electricity as its driving source. Therefore, it has environmental friendliness and energy-saving potentials. There are different types of adsorption systems such as single stage, two-stage and three-stage adsorption system. A basic conventional single stage adsorption system involves one condenser and one evaporator, and two beds, each having one heat exchanger. Moreover advanced single stage adsorption systems, such as two-bed mass recovery, three-bed, three-bed mass recovery, and heat recovery type were proposed. The performance of advance single stage systems is better than that of the basic two-bed adsorption system [1-3].

To reduce the temperature of the heat source, Saha et al. [4] proposed a design of a four-bed two-stage adsorption system. They showed numerically that their system can utilize effectively solar/wasted heat with temperature below 70 °C. Alam et al. [5] and Hamamoto et al. [6] identified the influence of design parameters and operating conditions on the performance of the system proposed by Saha. Moreover, the modification of the system in operation procedure such as re-heat scheme was investigated by Khan et al. [7-9], Alam et al. [10] and S.K. Farid et al. [11]. These investigations showed that the system can work with the heat source having the temperature as low as 45 °C but the coefficient of performance (COP) of two-stage adsorption system is lower than that of the advanced single-stage systems.

To enhance COP for the systems employing the heat source temperature around 45 °C, Saha et al. [12] proposed a design of advance three-stage system and investigated the effect of different parameters (e.g., cycle time, heat exchanger flow rate and temperature) on the system performance [13-14]. They showed that the three-stage adsorption system can work as low as 40 °C heat source temperature. It has three pairs of adsorber/desorber heat exchangers in each stage needing a larger volume in the system to make it workable at low temperature. To reduce the overall size, four-bed three-stage systems have been considered by Rahman et al. [15].

In this work an innovative design of the system has been proposed by adding one heat exchanger bed on the upper side of a four-bed three-stage system for conversion to a four-stage adsorption system. The prime intention is to utilize very low grade waste heat keeping the heat sink temperature fixed. Finally, the effect of cycle time on the system performance was investigated for different heat source temperature.

II. Description of Three-stage Adsorption Cycle

It is well known that a conventional single-stage adsorption cycle cannot be made operational when heat source temperature is below 60 °C with a coolant of temperature 30 °C or higher. For a practical utilization

of these temperatures in the adsorption system operation, two- or three-stage regeneration is necessary. This is because lower heat source temperature is not sufficient enough to drive vapour from the evaporator pressure to the condenser pressure. It was observed that a higher stage system can utilize lower heat source temperature. For example, a two-stage system can work as low as 45 ^{o}C while a three-stage system can work as low as 40 ^{o}C. The observed success of the stage-regeneration has led us to examine the four-stage system to utilize more lower temperature waste heat. The schematic diagram of the system is shown in Fig. 1 and its operation mode is given in Table 1. It consists of five adsorber/disorber heat exchanger beds, namely, Bed 1, Bed 2, Bed 3, Bed 4 and Bed 5, one condenser and one evaporator. Bed 1 and Bed 2 work as lower temperature and pressure (near to evaporator pressure) and Bed 5 works in upper temperature and pressure (near to condenser pressure). Bed 3 and Bed 4 work in two separate levels in between evaporator and condenser pressure level. Only Bed 1 and Bed 2 are connected with the evaporator and Bed 5, with the condenser. In first half cycle, Bed 3 adsorbs vapour from Bed 1 and then transfers to Bed 4 and finally to the condenser via Bed 5. Similarly, in second half cycle Bed 3 adsorbs vapour from Bed 2 and then transfers to condenser through Bed 4 and Bed 5. As a result, Bed 3, Bed 4 and Bed 5 are completing two full cycles, while Bed 1 and Bed 2 are completing only one full cycle operation at the same time of operation.

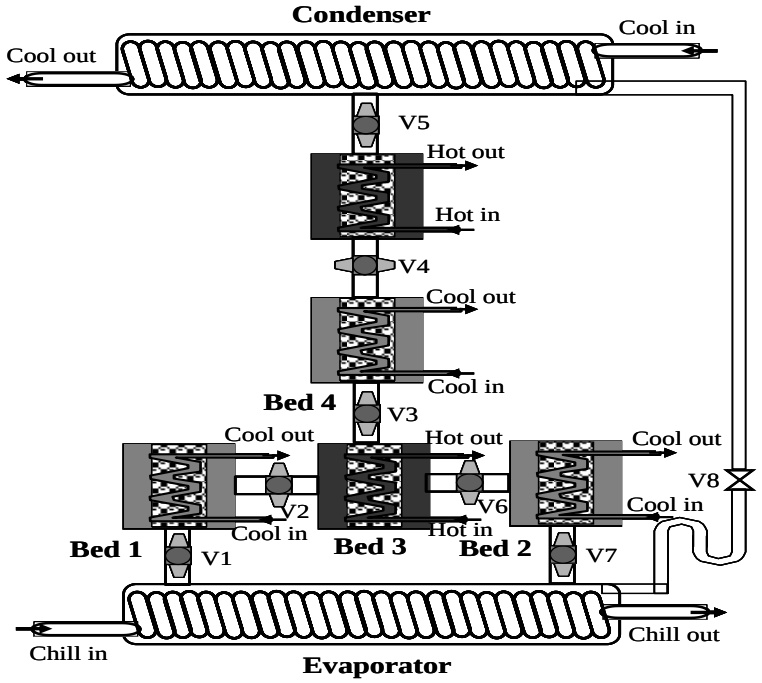

Fig. 1: Schematic diagram of proposed four-stage adsorption system.

The conceptual Dühring diagram of the proposed four-stage adsorption system is shown in Fig.2. The cyclic diagrams a-b-c-d-a, e-f-g-h-e, i-j-k-l-i and m-n-o-p-m indicate the four different stages (i.e., first, second, third and fourth stage) in between condenser and evaporator pressure level. Bed 1 and 2 work in first stage and other three beds work in three different stages. All beds are completing four thermodynamically modes, i.e., pre-heating, desorption, pre-cooling and adsorption modes, which are sequentially followed by the sides a-b, b-c, c-d and d-a, and e-f, f-g, g-h and h-e for Bed 1/2 and Bed 3, respectively. Similarly, the sides i-j, j-k, k-l and l-i, and m-n, n-o, o-p and p-m indicate the modes of pre-heating, desorption, pre-cooling and adsorption modes for Bed 4 and Bed 5, respectively. On the other hand, to complete a full cycle operation of the system, each bed is to complete 8 operational modes, namely A, B, C, D, E, F, G and H, which is shown in Table 1.

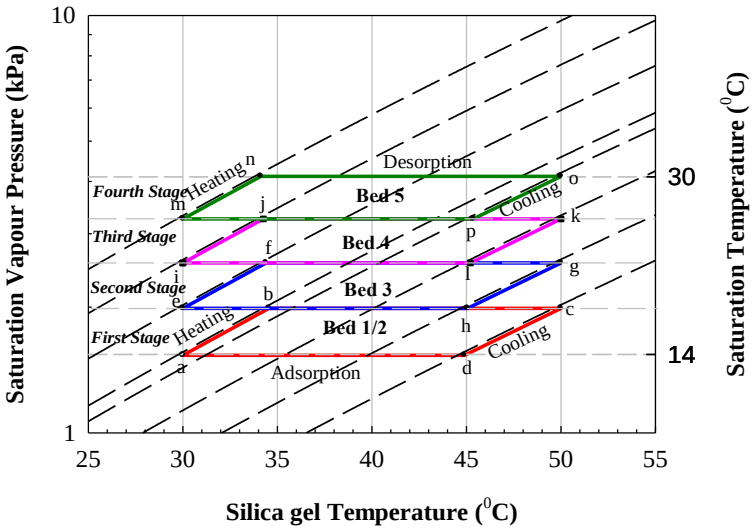

Fig.2: Conceptual Dühring diagram of proposed cycle.

Table 1: Operation mode and cycle time of four-stage adsorption system.

Mode	A τ_1	B τ_2	C τ_1	D τ_2	E τ_1	F τ_2	G τ_1	H τ_2
Bed 1	400	30	400	30	860			
Bed 2	1260					30	400	30
Bed 3	400	30	400	30	400	30	400	30
Bed 4	400	30	400	30	400	30	400	30
Bed 5	400	30	400	30	400	30	400	30

Adsorption | Pre-heating | Desorption | Pre-cooling

III. Simulation Methods and Materials

In the analysis, it is assumed that the temperature, pressure and refrigerant concentration throughout the adsorbent bed are uniform. The assumption is valid if the thermal conductivity of the bed is high. With the assumption, the energy balance of the system is explained in the following sections. The meaning of physical quantities can be found in nomenclatures following section 5.

3.1 Adsorption and desorption energy balance

The heat transfer and energy balance equations for the adsorption/desorption bed are given below:

$$T_{out}^{col/hot} = T^b + (T_{in}^{col/hot} - T^b).\exp\left(-\frac{(U.A)_{hex}^b}{\dot{m}_w^{col/hot}\cdot C_w}\right) \tag{1}$$

$$W_s^b C_s \frac{dT^b}{dt} + W_s^b C_w \frac{d(q^{ads/des}\cdot T^b)}{dt} + (W\cdot C)_{hex}^b \frac{dT^b}{dt} = \dot{m}_w^{col/hot} c_w (T_{in}^{col/hot} - T_{out}^{col/hot}) + W_s^b Q_{st} \frac{dq^{ads/des}}{dt} - \alpha.W_s^b C_{wv}\{\beta(T^b - T^e) + (1-\beta)(T^b - T_{wv})\}\frac{dq^{ads/des}}{dt} \tag{2}$$

Here, the heat transfer fluid temperatures, $T_{in}^{col/hot}$ and $T_{out}^{col/hot}$, denote, respectively, temperature of the cooling water upon adsorption and that of the hot water upon desorption. T^b stands for adsorption/desorption

bed temperature. Equations (1) and (2), used for adsorption and desorption purposes, are identical. Heat transfer is fully dependent on the heat transfer coefficient U^b_{hex} and heat transfer area A^b_{hex} of the bed. The left-hand side of Eq. (2) indicates either the amount of sensible heat required to cool during adsorption or heat the silica-gel (s), water (w) as well as metallic parts of the heat exchanger (hex) during desorption. The first term of right hand side stands for the total amount of heat released to the cooling water upon adsorption or provided by the hot water upon desorption, the second term for the adsorption heat release or desorption heat input and the last two terms for the sensible heat of the adsorbed vapour. α is either 0 or 1 depending on whether bed is working as desorber or adsorber and β is either 1 or 0 depending on whether bed is connected with evaporator or other bed. Heat balance expression in Eq. (2) does not consider the external heat losses to the environment.

3.2 Evaporator energy balance

The heat transfer and energy balance equations of evaporator are given below:

$$T^{chil}_{out} = T^e + (T^{chil}_{in} - T^e).\exp\left(-\frac{(U\cdot A)^e_{hex}}{\dot{m}^{chil}_w \cdot C_w}\right) \tag{3}$$

$$(W^e_w C_w + (W\cdot C)^e_{hex})\frac{dT^e}{dt} = -L_w W^b_s \frac{dq^{ads}}{dt} - W^b_s C_w (T^c - T^e)\frac{dq^{des}}{dt} + \dot{m}^{chil}_w c_w (T^{chil}_{in} - T^{chil}_{out}) \tag{4}$$

Here, A^e_{hex} and U^e_{hex} are, respectively, the heat transfer area and heat transfer coefficient of evaporator and L_w is the latent heat of vaporization.

3.3 Condenser energy balance

The heat transfer and energy balance equations of the condenser are as follows:

$$T^{c,col}_{out} = T^c + (T^{c,col}_{in} - T^c).\exp\left(-\frac{(U\cdot A)^c_{hex}}{\dot{m}^{c,col}_w \cdot C_w}\right) \tag{5}$$

$$(W^c_w C_w + (W\cdot C)^c_{hex})\frac{dT^c}{dt} = \{-L_w - C_{wv}(T^b - T^c)\}W^b_s \frac{dq^{des}}{dt} + \dot{m}^{c,col}_w c_w (T^{c,col}_{in} - T^{c,col}_{out}) \tag{6}$$

Here, A^c_{hex} and U^c_{hex} are, respectively, the heat transfer area and heat transfer coefficient of the condenser.

3.4 Adsorption and desorption rate

The adsorption/desorption rate can be expressed as

$$\frac{dq^{ads/des}}{dt} = ksap(q^* - q^{ads/des}) \tag{7}$$

where the overall mass transfer coefficient (ksap) for adsorption is given by

$$ksap = 15\cdot D_S/(R_p)^2. \tag{8}$$

Here, R_p denotes the average radius of silica gel particle. The adsorption rate is controlled by surface diffusion inside gel particle and surface diffusivity (D_S), which can be expressed by Arrhenius equation as a function of temperature as

$$D_S = D_{so}\exp\left(\frac{-E_a}{R\cdot T}\right) \tag{9}$$

where D_{so} is a pre-exponential term whose value is taken as $2.54\text{x}10^{-4}$ m^2 s^{-1}; E_a denotes the activation energy; R represents the gas constant and T stands for temperature. q^* in Eq. (7) is the adsorption uptake at equilibrium state that can be expressed [16] as

$$q^* = \frac{0.8\times[P_s(T_w)/P_s(T_s)]}{1+0.5\times[P_s(T_w)/P_s(T_s)]}\ . \tag{10}$$

Here, $P_s(T_w)$ and $P_s(T_s)$ are the saturation vapour pressures at temperatures T_W of the water vapour and T_S of the silica gel, respectively. Antoine correlates the saturation pressure and temperature, which can be expressed as

$$P_s = 133.32 \times \exp(18.3 - 3820\ /(T - 46.1)) \tag{11}$$

3.5 Mass balance

Total mass of refrigerant of the system is assumed constant. The rate of change of the mass of liquid refrigerant can be expressed through the following equation:

$$\frac{dW_w^e}{dt} = -W_s^b \left(\frac{dq^{des-con}}{dt} + \frac{dq^{ads-evp}}{dt} \right). \tag{12}$$

Here, W_s^b is the weight of silica gel packed in each bed and W_w^e is the weight of refrigerant in the liquid phase. The supercripts ‘‘des-con’’ and ‘‘ads-evp’’ stand for the vapor flows, respectively, from the desorber to the condenser and evaporator to adsorber. In this case, vapour transfer of Bed 3 is not taken into account. It is assumed that it has desorbed all refrigerant vapour whatever adsorbed by it.

3.6 System performance

The performance of four-stage adsorption cycle is mainly characterized by specific cooling power (SCP), which is the cooling capacity per unit mass of adsorbent and coefficient of performance (COP) The latter is the ratio of the heat released by the evaporator to the heat source input to the bed. SCP and COP can be calculated by using the following equations:

$$SCP = \dot{m}_w^{chil} C_w \int_0^{t_{cycle}} (T_{in}^{chil} - T_{out}^{chil}) dt \,/\, t_{cycle} W_{s,tot}\ , \tag{13}$$

and

$$COP = \frac{\dot{m}_w^{chil} C_w \int_0^{t_{cycle}} (T_{in}^{chil} - T_{out}^{chil}) dt}{\dot{m}_w^{hot} C_w \int_0^{t_{cycle}} (T_{in}^{hot} - T_{out}^{hot}) dt}. \tag{14}$$

Here, t_{cycle} and $W_{s,tot}$ indicate the total cycle time and total mass of adsorbent of the system, respectively.

3.7 Simulation procedure

A complete simulation program has been developed using MATLAB software to solve the above mentioned equations. Adsorption/desorption rate equation, energy balance equation of beds, condenser and evaporator, and mass balance equation have been solved simultaneously using MATLAB ode45 solver. All input parameters such as adsorbent-refrigerant properties, flow rates of heat transfer fluids and heat exchangers specifications have been assigned such initial values that the system cyclic operation can be continued.

IV. Results and Discussion

The simulation program developed for proposed system has been operated by adopting the basic input parameters and standard working conditions as presented in Table 2 [17]. The variation of water contents in adsorber/desorber beds with cycle time at the heat source temperature of 50 ^{o}C is shown in Fig. 3. It is obvious from this figure that the water contents are increased during the adsorption time (i.e., mode E-H-A for Bed 1, mode A-E for Bed 2, mode C with G for Bed 3, mode A with E for Bed 4 and mode C with G for Bed 5) and are decreased during the desorption time (i.e., mode C for Bed 1, mode G for Bed 2, mode A with E for Bed 3, mode C with G for Bed 4 and mode A with E for Bed 5). During pre-cooling and pre-heating time beds are fully disconnected from other parts of the system. Therefore, the water contents remain constant in the modes B, D, F and H for Bed 3, 4 and 5.

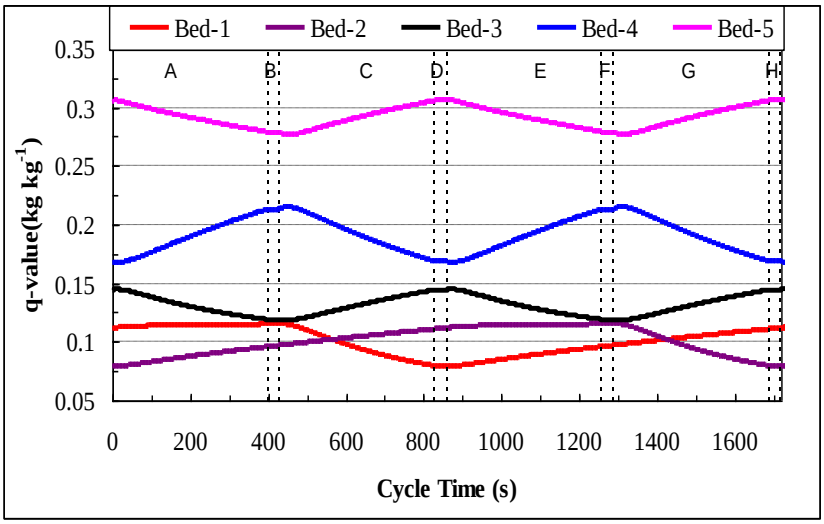

Fig. 3: Variation of water content in beds with cycle time at 50 ^{o}C heat source temperature.

Table 2: Basic input parameters and standard working conditions

Parameters	Value	Unit
Q_{st}	2.80×10^{6}	J kg^{-1}
E_a	4.2×10^{4}	J mol^{-1}
D_{so}	2.54×10^{-4}	m^2 s^{-1}
R	8.314	J mol^{-1} K^{-1}
R_p	0.30×10^{-3}	M
C_w	4.18×10^{3}	J kg^{-1} K^{-1}
C_{wv}	1.89×10^{3}	J kg^{-1} K^{-1}
L_w	2.50×10^{6}	J kg^{-1}
C_{Cu}	386.00	J kg^{-1} K^{-1}
C_{Al}	905.00	J kg^{-1} K^{-1}
C_s	924.00	J kg^{-1} K^{-1}
A_{hex}^{b}	0.61×16	m^2
A_{hex}^{e}	3.00	m^2
A_{hex}^{c}	1.00	m^2
U_{hex}^{c}	3900.00	W m^{-2} K^{-1}
U_{hex}^{b}(desorption)	750.00	W m^{-2} K^{-1}
U_{hex}^{b}(adsorption)	1000.00	W m^{-2} K^{-1}
U_{hex}^{e}	5800.00	W m^{-2} K^{-1}
W_s^{b}	16.00	Kg
W_{hex}^{b} (Cu)	12.67	Kg
W_{hex}^{b}(Al)	16.87	Kg
W_{hex}^{e}	2x4.8	Kg
W_w^{e}	61.32	Kg
W_w^{c}	24.98	Kg
W_{hex}^{c}	12.80	Kg
Standard working condition		
T_{in}^{hot}	35 - 85	^{o}C
$\dot{m}_w^{hot}$	1.0	kg s^{-1}

T_{in}^{col}	30	^{o}C
$\dot{m}_{w}^{col}$	1.0	kg s^{-1}
$T_{in}^{c,col}$	30	^{o}C
$\dot{m}_{w}^{c,col}$	0.8	kg s^{-1}
T_{in}^{chil}	14	^{o}C
$\dot{m}_{w}^{chil}$	0.3528	kg s^{-1}

Temperature profile for all adsorbent beds, condenser and evaporator is shown in Fig.4. It is observed that during the adsorption stages, the bed temperatures at first sharply decrease and then become saturated, since the beds are cooled by cooling water. On the other hand, during the desorption times, the bed temperatures at first sharply increase after that it become saturated due to heating by hot water. Similarly, during the pre-heating and pre-cooling stages bed temperatures are sharply increased and decreased, respectively. The condenser temperature is increased only during the desorption time of Bed 5 due to vapour transfer from bed to condenser, whereas the evaporator temperature stays nearly constant with cycle time. In Table 1 it is clear that either Bed 1 or Bed 2 are always connected to the evaporator and produces continuous cooling supply. Consequently it is observed that the proposed cycle keeps constant evaporator temperature with less fluctuation.

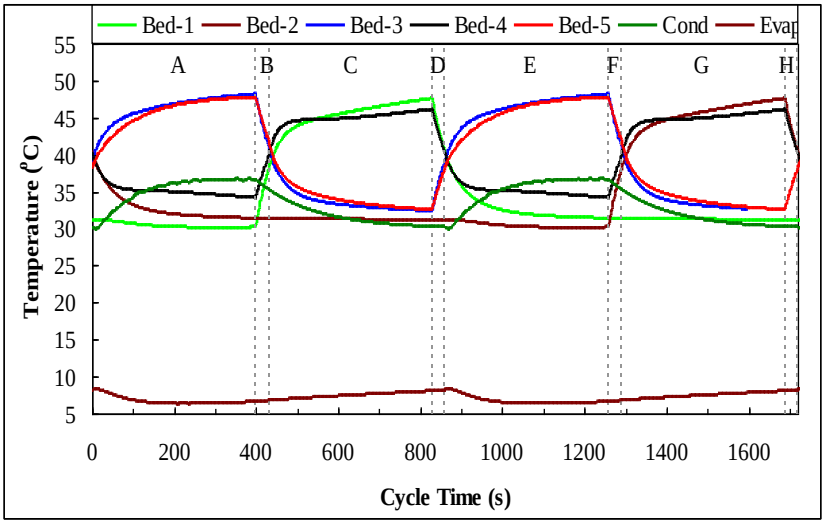

Fig. 4: Temperature profile of beds, condenser and evaporator at 50 ^{o}C heat source temperature.

Effect of total cycle time on the system performance is investigated at 50 ^{o}C heat source temperature, which is shown in Fig. 5. In this case only the desorption time, τ_1 is increased from 50 s to 1000 s whereas the pre-cooling/pre-heating time, τ_2 is kept constant at 30 s. It is obvious that initially SCP is increased with cycle time after that it gets decreased. Similar effect of the total cycle time is observed on COP. Maximum performance is observed at the cycle time 1720 s. This cycle time is chosen for investigating the effect of heat source temperature on the system performance.

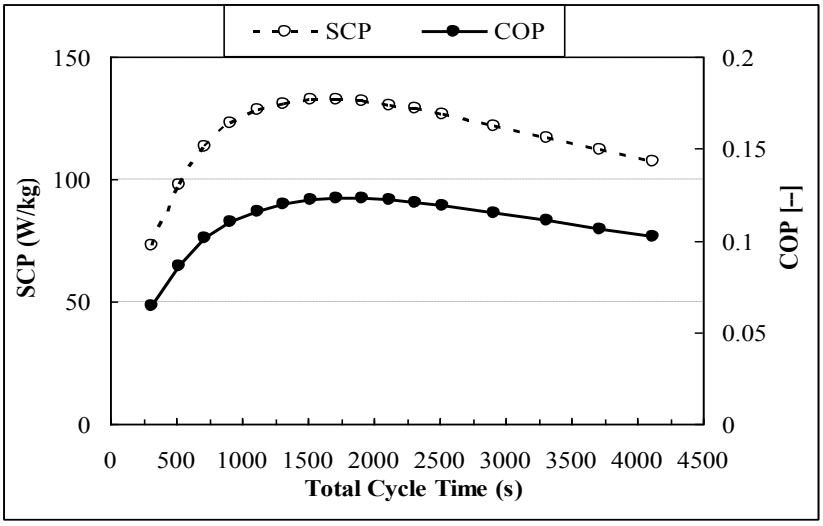

Fig. 5: Effect of total cycle time on the system performance at 50 ^{o}C heat source temperature.

The performance of the proposed system at different heat source temperature is shown in Fig. 6. It is apparent that the system can work at very low temperature as low as 35 ^{o}C with a coolant temperature at 30 ^{o}C. The SCP is increased with the increase of heat source temperature whereas COP is increased sharply with heat source temperature up to 50 ^{o}C and then it decreases with temperature. The maximum COP is found to be 0.12 at 50 ^{o}C heat source temperature whereas both SCP and COP are very low at lowest temperature. An increase of heat source temperature with a fixed heat sink causes the system to increase the amount of refrigerant adsorption/desorption promptly, resulting in a higher SCP at higher heat source temperature. Due to a similar reason chilled water outlet temperature is decreased with heat source temperature, which is shown in Fig. 7. In this case, the total cycle time and the flow rate of chilled water are kept constant whereas only heat source temperature is varied from 35 ^{o}C to 90 ^{o}C.

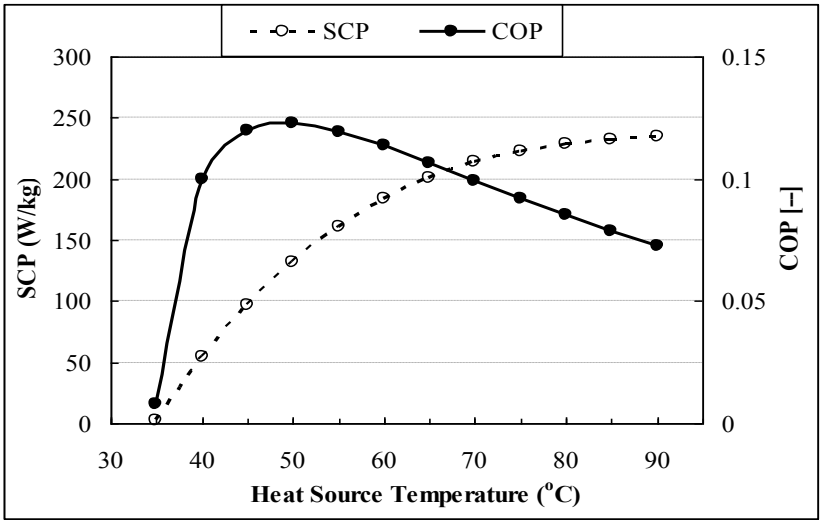

Fig. 6: Variation of SCP and COP of proposed cycle with heat source temperature.

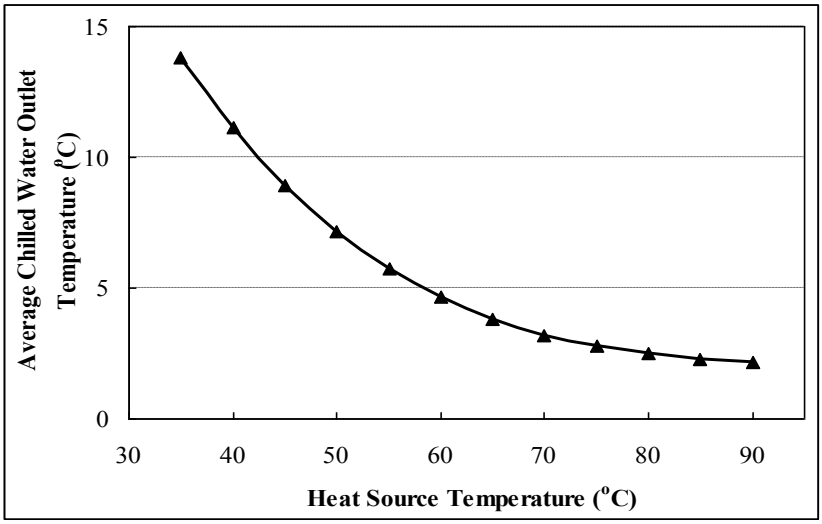

Fig. 7: Variation of average chilled water outlet temperature with heat source temperature.

V. Conclusion

An innovative design of a four-stage adsorption system is introduced. A simulation program has been developed to investigate the performance of the system for different heat source temperature and cycle time. Maximum performance of the system has been observed when cycle time is 1720 s. The cycle is effectively applicable to utilize waste heat source from 35 ^{o}C to 90 ^{o}C temperature. It is found that the specific cooling power of the proposed cycle increased with heat source temperature. The maximum coefficient of performance of the system is observed to occur at the 50 ^{o}C temperature.

Nomenclatures

A	area (m^2)
C	specific heat (J kg^{-1} K^{-1})
D_{so}	surface specific heat (m^2 s^{-1})
E_a	activation energy (J kg^{-1})
L	latent heat of vaporization (J kg^{-1})
$\dot{m}$	mass flow rate (kg s^{-1})
P	saturated vapour pressure (Pa)
q	fraction of refrigerant that can be adsorbed by the adsorbent (kg kg^{-1})
q*	fraction of refrigerant that can be adsorbed by the adsorbent under saturation condition (kg kg^{-1})
Q_{st}	isosteric heat of adsorption (J kg^{-1})
R	gas constant (J kg^{-1} K^{-1}))
R_p	average radius of silica gel particles (m)
T	temperature (K)
t	time (s)
U	overall heat transfer coefficient (W m^{-2} K^{-1})
W	mass (kg)
Cool	cooling water
Hot	hot water
V	valve

Superscripts

b	adsorption/desorption bed
c	condenser
e	evaporator
ads	adsorption
des	desorption
col	cooling water
hot	hot water
chil	chilled water

Subscripts

hex	heat exchanger (Copper and Aluminium)
in	inlet

out	outlet
s	silica gel
tot	total
cycle	total cycle
w	water
wv	water vapour

References

[1.] Akahira A., Alam K.C.A., Hamamoto Y., Akisawa A., Kashiwagi T., 2005, Experimental investigation of mass recovery adsorption refrigeration cycle, Int. J. Refrigeration, 28,565-572.

[2.] Khan M.Z.I., Saha B.B., Alam K.C.A., Akisawa A. and Kashiwagi T., 2007. 'Study on solar/waste heat driven multi-bed adsorption chiller with mass recovery', Renewable Energy, 32, 365-381.

[3.] Uyun A.S., Akisawa A., Miyazaki T., Ueda Y. and Ksahiwagi T., 2009. Numerical analysis of an advanced three-bed mass recovery adsorption refrigeration cycle, Applied Thermal Engineering, 29, pp. 2876-2884.

[4.] Saha B.B., Akisawa A. and Kashiwagi T., 2001. Solar/waste heat driven two-stage adsorption chiller: the prototype. Renewable Energy 23, 93-101.

[5.] Alam K. C. A., Saha B. B., Akisawa A. and Kashiwagi T., 2004. Influence of design and operating conditions on the system performance of a two stage adsorption chillier. Chem. Eng. Commun. 191, 981-997.

[6.] Hamamotoa Y., Alam K.C.A., Akisawa A. and Kashiwagi T., 2005. Performance evaluation of a two-stage adsorption refrigeration cycle with different mass ratio. Int. J. Refrigeration 28, 344-352.

[7.] Khan M.Z.I., Saha B.B., Miyazaki T., Akisawa A. and Kashiwagi T., 2005. Study on a two stage adsorption chiller using re-heat. Proceedings of JSRAE annual conference-10.,Tokyo, Japan, 23-27.

[8.] Khan M.Z.I., Alam K.C.A., Sahab B.B., Hamamoto Y., Akisawaa A. and Kashiwagi T., 2006. Parametric study of a two-stage adsorption chiller using re-heat-the effect of overall thermal conductance and adsorbent mass on system performance. Int. J. therm. Sci. 45, 511-519.

[9.] Khan M.Z.I., Alam K.C.A., Saha B.B., Akisawa A., Kashiwagi T., 2007. Study on a re-heat two-stage adsorption chiller - the influence of thermal capacitance ratio, overall thermal conductance ratio and adsorbent mass on system performance. Appl. Therm. Eng. 27, 1677-1685.

[10.] Alam K.C.A., Khan M.Z.I., Uyun A.S., Hamamoto Y., Akisawa A., Kashiwagi T., 2007. Experimental study of a low temperature heat driven re-heat two stage adsorption chiller. Appl. Therm. Eng. 27, 1686-1692.

[11.] Farid S.K., Billah M.M., Khan M.Z.I., Rahman M.M. and Sharif U. M., 2011. A numerical analysis of cooling water temperature of two-stage adsorption chiller along with different mass ratios. Int. Commun. Heat Mass Transfer 38, 1086-1092.

[12.] Saha B.B, Boelman E.C. and Kashiwagi T., 1995. Computational analysis of an advanced adsorption-refrigeration cycle. Energy 20 (10), 983-994.

[13.] Saha, B. B., Akisawa, A., and Kashiwagi T., 1997. Silica gel water advanced adsorption refrigeration cycle. Energy 22(4), 437-447.

[14.] Saha B.B., Koyama S., Kashiwagi T., Akisawa A., Ng K.C., Chua H.T., 2003. Waste heat driven dual-mode, multi-stage, multi-bed regenerative adsorption system. Int. J. Refrigeration 26, 749-757.

[15.] Rahman A.F.M. M., Ueda Y., Akisawa A., Miyazaki T., Saha B.B., 2013. Design and Performance of an Innovative Four-bed, Three-Stage Adsorption Cycle. *Energies* 2013, *6*, 1365-1384.

[16.] Akahira A., 2004. Research on the Advanced Adsorption Refrigeration Cycles with Vapour Recovery. Ph.D. Thesis, Tokyo University of Agriculture and Technology, Tokyo, Japan.

[17.] Moriyama K., 2007. Performance Improvement of Adsorption Chillers by the Optimization of Cycle time Component. MS thesis, Tokyo University of Agriculture Technology, Tokyo, Japan.